ChemComm

Chemical Communications

Accepted Manuscript

ROYAL SOCIETY OF CHEMISTRY

rsc.li/chemcomm

COMMUNICATION

Simple and Robust Polymer-based Sensor for Rapid Cancer Detection using Serum

Received 00th January 20xx,
Accepted 00th January 20xx

DOI: 10.1039/x0xx00000x

Ngoc D. B. Le, [a] Arvind K. Singla, [b] Yingying Geng, [a] Jinsong Han, [c] Kai Seehafer, [c] Gyan Prakash, [a] Daniel F. Moyano, [a] Charlene M. Downey, [b] Michael J. Monument, [d] Doha Itani, [e] Uwe H. F. Bunz, [c] Frank R. Jirik, [b] and Vincent M. Rotello *[a]

We report a polymer-based sensor that rapidly detects cancer based on changes in serum protein levels. Using three ratiometric fluorescence outputs, this simple system identifies early stage and metastatic lung cancer with a high level of accuracy exceeding many biomarker-based assays, making it an attractive strategy for point-of-care testing.

Effective treatment of cancer requires early detection, making the creation of rapid and inexpensive sensing systems important for both health and healthcare cost reasons.[1] Serum presents a minimally invasive target for the design of cancer diagnostics. A broad range of protein level in serum changes during tumor development.[1b,2] Most techniques developed for cancer detection using serum focus on specific biomarkers. Enzyme linked immunosorbent assay (ELISA) remains the method of choice.[3] However, it has limitations in sensitivity for low abundance biomarkers. Most importantly, many cancer types do not have ideal biomarkers, due to widely different baseline expressions of targeted biomarkers in the population, often leading to false positives and negatives.[1a,4] Serum analysis can also be done by gel electrophoresis coupled with mass spectrometry, but analysis time, quantification challenges, and expensive instrumentation are an issue.[5]

Array-based 'chemical noses' provide an alternative to biomarker-based sensing which do not require previous knowledge of the analytes; instead the selective interactions between sensor elements and analytes will generate a unique fingerprint for each analyte. Through pattern recognition, the identity of the target analyte can be further determined. This property makes array-based sensing a powerful tool in sensing complex biological systems. Previously an array of five gold nanoparticles has been shown to detect proteins in human serum.[7] Overall, chemical noses can identify proteins,[7] carbohydrates,[8] and mammalian cells[9] in addition to white wines, fruit juices and non-steroidal anti-inflammatories.[10]

Simplicity and scalability are important attributes for point-of-care (POC) diagnostics.[11] To address this concern, we focus on a simple but robust polymer-based sensor system for profiling serum for cancer diagnostics. This system is based on the fluorescence signals of two charge-complementary conjugated polymers and their fluorescence resonance energy transfer (FRET) to provide three ratiometric outputs. This polymer-only platform utilizes the structural diversity, fluorescence efficiency, stability, and scalability of conjugated polymer "molecular wires"[12] to detect cancer in sera of cancer-bearing mice. In this study transgenic and xenograft models were selected to plausibly recapitulate some of the clinically-relevant events seen in patients with stage 1 and stage 4 lung cancer, respectively. Our polymer-based sensor achieved a high level of accuracy in identifying both advanced and early stage of cancer, exceeding standard single biomarker diagnostic tests.[13]

We designed two different backbones for the donor and acceptor polymers to provide an optimum FRET-based sensor, which is composed of polyfluorene sulfonate (PFS) and poly(p-phenyleneethynylen) (PPEs), respectively. Upon addition of serum, the fluorescence of each polymer and their FRET process are modulated due to the binding of serum proteins to the polymers. These fluorescence fingerprints are then analyzed by linear discriminant analysis (LDA) to create a reference set and predict future unknown samples (Scheme 1). Upon excitation at the PFS absorbance of 356 nm, the complexes PFS-PPE1 and PFS-PPE2 exhibit efficient FRET, with a decreased fluorescence emission at 420 nm and increased emission at 480 nm for PPE1 and 482 nm for PPE2 (Fig. S1).

[a] *Department of Chemistry, University of Massachusetts Amherst, 710 N. Pleasant St., Amherst MA 01003, U.S.A.*
[b] *Department of Biochemistry and Molecular Biology, The McCaig Institute for Bone and Joint Health, University of Calgary, 2500 University Drive NW, Calgary, Alberta T2N 4N1, Canada.*
[c] *Organisch-Chemisches Institut, Ruprecht-Karls-Universität Heidelberg, Im Neuenheimer Feld 270, 69120 Heidelberg, Ger-many.*
[d] *Department of Surgery, The McCaig Institute for Bone and Joint Health, Arnie Charbonneau Cancer Institute, University of Calgary, 2500 University Drive NW, Calgary, Alberta T2N 4N1, Canada.*
[e] *Department of Pathology and Laboratory Medicine, Calgary Laboratory Services/University of Calgary, 2500 University Drive NW, Calgary, Alberta T2N 4N1, Canada.*
Electronic Supplementary Information (ESI) available: [details of any supplementary information available should be included here]. See DOI: 10.1039/x0xx00000x

COMMUNICATION

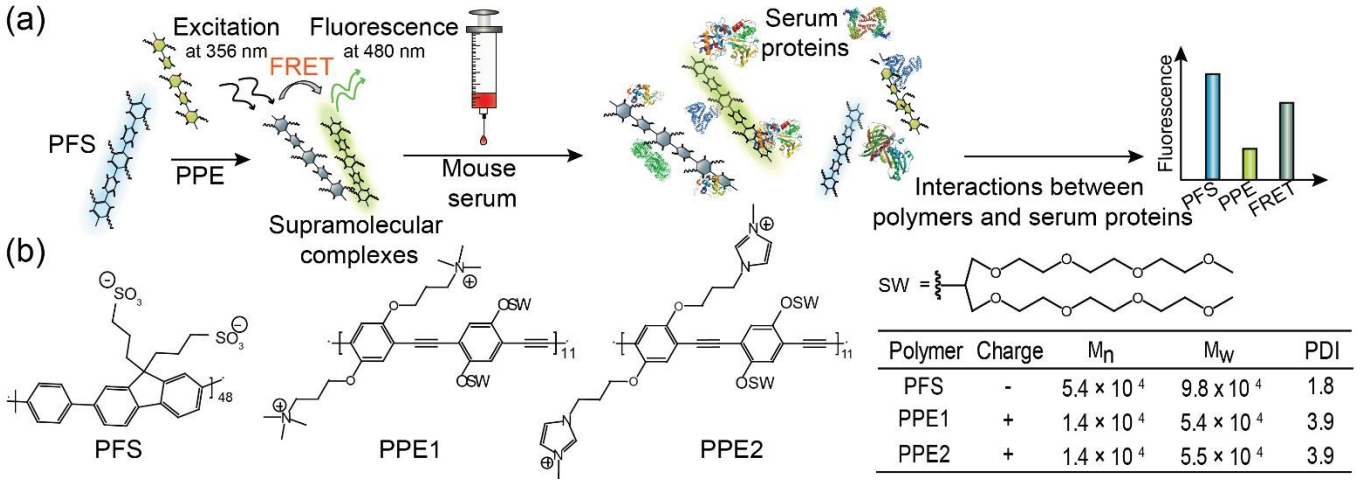

Polymer	Charge	M_n	M_w	PDI
PFS	-	5.4×10^4	9.8×10^4	1.8
PPE1	+	1.4×10^4	5.4×10^4	3.9
PPE2	+	1.4×10^4	5.5×10^4	3.9

Scheme 1. Schematic illustration of FRET-based polymer sensor for serum sensing. (a) Two polymers with opposite charges form supramolecular complexes, generating FRET responses. The fluorescence intensities of the three channels are interfered by serum proteins. (b) Chemical structures and characteristics of polymers used. Mn: number-average molecular weight; Mw: weight-average molecular weight; PDI: polydispersity index.

After determining the ratio of PFS and PPEs with a suitable FRET response (Fig. S2), each pair was tested in calf serum, the addition of which caused a decrease in PPE fluorescence and an increase in PFS fluorescence (Fig. 1a). This observation indicated a dissociation of the complexes upon binding with serum proteins. These FRET-based sensors further identifed eight proteins dissolved in phosphate buffer saline (PBS) (Table S1). We observed distinct fluorescence changes for all eight proteins from each polymer pair (Fig. S3). LDA plots showed correct classifications of 100 % and 97.0 %, respectively. In addition, both sensors successfully identified unknown samples (98.4 % and 89.0 %, respectively) in a matter of minutes (Fig. 1b, d).

Limit of detection is a crucial measurment for early stage of cancer, therefore, we further validated both sensors using a more challenging test bed: cancer-bearing mice from a transgenic lung model, established by mutations in the *Kras* and *p53* genes (Table S2). After determining the total amount of serum proteins necessary for the assay, four different concentrations of normal and cancerous sera were prepared and titrated with each sensor. The LDA plot showed separation of normal (upper) versus cancerous (lower) serum samples with a shift from left to right that associates with low to high concentrations of total proteins: 1, 5, 10, and 20 mg/ml (Fig.1c). Due to its stable and differentiable fluorescence responses, we chose 5 mg/ml for further experiments. Both sensors were able to classify all 8 clusters of 64 serum samples (4 concentrations × 2 serum types (normal and cancerous) × 8 replicates). Since PFS-PPE1 performed better than PFS-PPE2 with 89.1 % versus 12.5 % (Fig. 1d) in unknown identification, we chose the PFS-PPE1 for all of our following experiments.

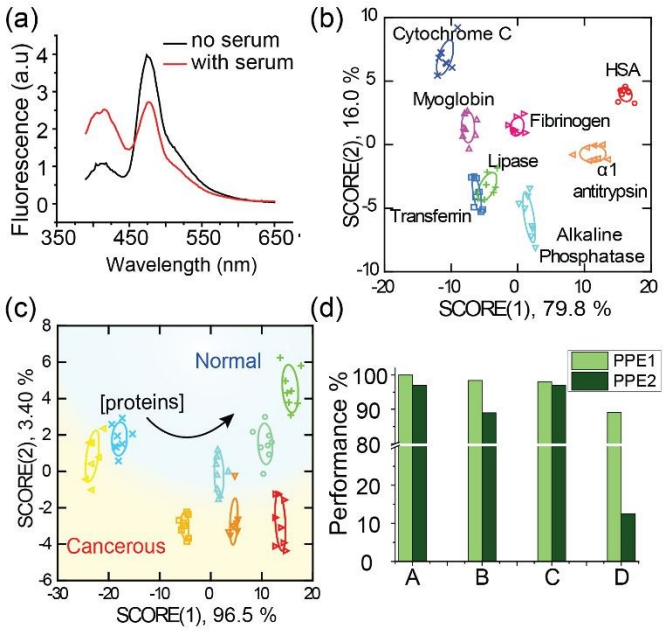

Fig. 1 Performance of PFS-PPE1 and PFS-PPE2 in classifying proteins in buffer and serum. (a) Fluorescence spectrum of PFS-PPE1 with or without calf serum. (b) LDA plot of the PFS-PPE1 responses to eight proteins in PBS at 10 μg/ml. HSA is Human Serum Albumin. First two canonical scores were plotted with 95% confidence ellipses. (c) Limit of detection of PFS-PPE1 in detecting normal and cancerous serum at 1, 5, 10, and 20 mg/ml protein concentrations, in the order from left to right. (d) Performance comparison between PFS-PPE1 and PFS-PPE2, where A is the classification accuracy of eight proteins in PBS, B is the correct unknown identification (CUI%) of these eight proteins, C is the classification accuracy of normal and cancerous mouse serum at different concentrations, and D is the CUI % of these serum samples.

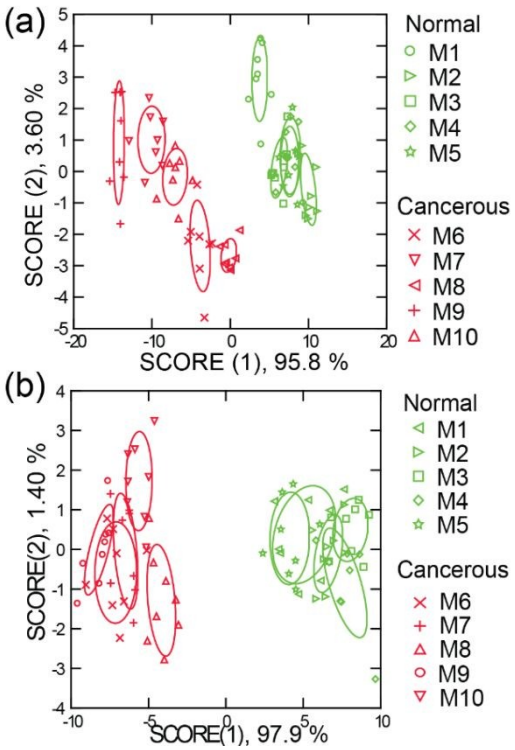

Fig. 2 Detection of mouse serum samples from (a) experimental lung cancer (stage 4) and (b) transgenic lung cancer model (stage 1) using PFS-PPE1. LDA plot of five normal and five cancerous mice. Two canonical scores were plotted with 95% confidence ellipses.

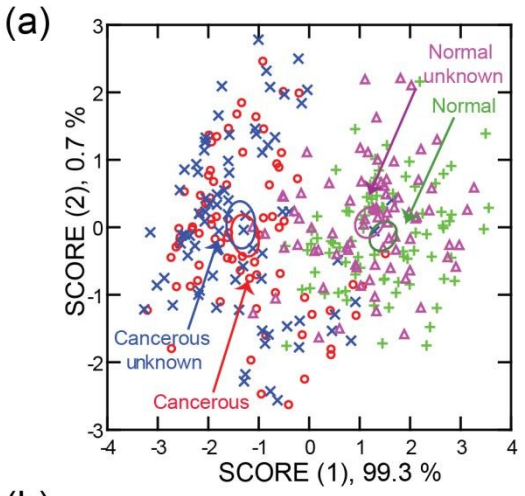

(b)

Model	True ID	# Samples	Correctly identified	Accuracy %
Transgenic Experimental	Cancer	80	73	91
Transgenic Experimental	Normal	80	66	83
TOTAL		160	139	**87**

Fig. 3 Combined serum data from transgenic (Stage 1) and experimental (Stage 4) lung models. (a) LDA plot of the PFS-PPE1 responses to cancerous and normal serum samples. (b) Unknown mouse serum samples were clustered with the established reference, resulted in an 87 % CUI.

One challenge in cancer diagnostics is that serum protein levels vary from patient to patient even within the same type of cancer.[14] This motivates us to examine the effect of individual differences from cancer-bearing mice of the same cancer model. We first used serum samples collected from a metastatic lung tumor model induced by H1299-EGFP-luc2 cells, representing stage 4 of lung cancer. We prepared and sensed five healthy controls (M1 to M5) and five cancerous mice (M6 to M10). The LDA plot shows distinct clusters for the control versus cancerous groups, with all five healthy controls and all five cancerous mice clustering together within their respective groups. The correct classification accuracy was 100 % (Fig. 2a). To test the reproducibility of our PFS-PPE1 sensor, we generated 80 blinded cases (5 mice × 2 types (normal and cancerous) × 8 replicates) for unknown prediction. 98.7 % of correct unknown identification was achieved (Fig. S4).

Promopt by the promising sensing results from the experimental mouse model, we further tested if our sensor could detect the early stage of cancer by using a transgenic lung model of mice bearing mutations in *Kras* and *p53* genes (representing stage 1 of lung cancer). This model also included five healthy and five cancerous mice. Similar to the metastatic tumor model, complete discrimination between normal and cancerous mice was also observed, demonstrating the sensitivity of the FRET pair in detecting early stage of cancer (Fig. 2b, Fig. S4). Interestingly, our sensor also picked up the heterogeneity in different cancerous mice, with more variations among cancerous samples than the normal controls in both models.

The ultimate goal of a diagnostic test is to know whether or not the patient has cancer. For this purpose, we combined data from both transgenic and experimental lung models to serve as the reference set. Due to the combination of data sets from two different disease models, more data scattering was observed. LDA showed 91 % of accurate classification between normal and cancerous samples with an effective correct unknown prediction of 87 % (Fig. 3).

To further evaluate the performance of LDA used in this study, we employed the receiver operating characteristic (ROC) curve, a standard method to access the performance of diagnostic tests.[15] Conventionally, the performance of a diagnostic test is reflected by two types of errors: true-positive rate (TPR) and false-positive rate (FPR). An ideal diagnostic test would have the TPR of one and the FPR of zero, giving an area under the curve (AUC) to be 1.0. A distribution of normal and cancerous serum samples from both models is shown in Figure 4a. ROC analysis performed on the combined data showed an AUC of 0.95 (95 % confidence level: 0.92-0.98) (Fig. 4b). The AUC value obtained here is well within the excellent diagnostic accuracy range (0.9-1.0).[16] Our test is also well above the standard accuracy range required for most diagnostic tests and is more accurate compared to most tests using single specific biomarker.[13]

In summary, we demonstrated a robust FRET-based polymer sensor that rapidly differentiated healthy and cancer-bearing mice using their sera. Serum samples from early stage cancer were accurately and readily identified, suggesting a potential application in early cancer detection. In addition, this

sensor benefits from the highly responsive conjugated fluorescent polymers as well as the simplicity of minimal two sensor elements. The stability and scalability of this polymer-based sensor make it an attractive strategy for point-of-care testing with a high level of accuracy compared to specific single biomarker tests.[11] More importantly, serum is an easily accessible biofluid, which allows a simple diagnostic and prognostic approach that poses low level of inconvenience to patients.

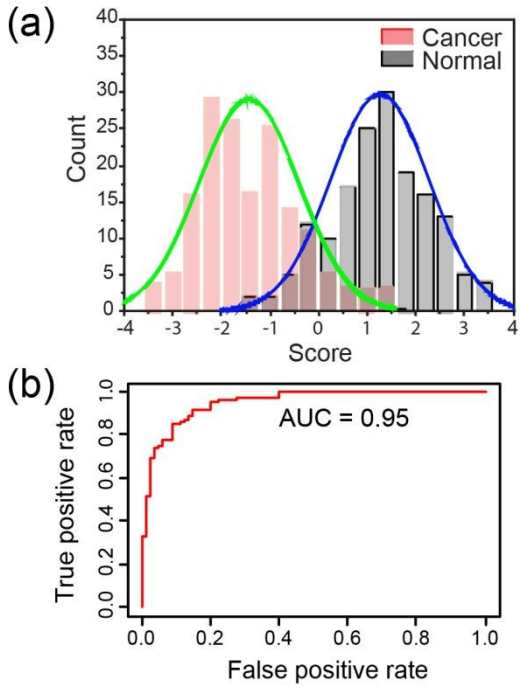

Fig. 4 Evaluating the capability of polymer-based sensor in cancer identification using combined data from both transgenic and experimental lung models. (a) Histogram of combined serum samples using LDA scores. (b) Receiver operating characteristic (ROC) analysis of the diagnostic test with AUC of 0.95,significantly higher than the clinical standard of 0.9 AUC.

V.M.R. acknowledges support from the NIH (GM077173) and the NSF (CHE-18081991). F.R.J. was the recipient of a Canadian Cancer Society Research Institute grant, with funds raised by the Canadian Cancer Society. Y.G. was partially supported by National Research Service Award T32 (GM008515) from the National Institutes of Health. The authors thank Ngoc Hong Thai for her assistance in ROC analysis.

Conflicts of interest

There are no conflicts to declare.

References

1 (a) J. Zhu, D. Djukovic, L. Deng, H. Gu, F. Himmati, E. G. Chiorean and D. Raftery, *J. Proteome Res.*, 2014, ***13***, 4120–4130; (b) A. B. Chinen, C. M. Guan, J. R. Ferrer, S. N. Barnaby, T. J. Merkel and C. A. Mirkin, *Chem. Rev.*, 2015, ***115***, 10530–10574.

2 (a) S. S. Aćimović, M. A. Ortega, V. Sanz, J. Berthelot, J. L. Garcia-Cordero, J. Renger, S. J. Maerkl and M. P. Kreuzer, R. Quidant, *Nano Lett.*, 2014, ***14***, 2636–2641; (b) P. M. Kosaka, V. Pini, J. J. Ruz, R. A. da Silva, M. U. González, D. Ramos, M. Calleja and J. Tamayo, *Nat. Nanotechnol.*, 2014, ***9***, 1047–1053.

3 (a) H. Lilja, D. Ulmert and A. J. Vickers, *Nat. Rev. Cancer*, 2008, ***8***, 268–278; (b) S. F. Kingsmore, *Nat. Rev. Drug Discov.*, 2006, ***5***, 310–321.

4 (a) A. Fernandez-Olavarria, R. Mosquera-Perez, R. Diaz-Sanchez, M. Serrera-Figallo, J. Gutierrez-Perez and D. Torres-Lagares, J. Clin. Exp. Dent., 2016, 8, e184-e193; (b) Y. E. Choi, J. W. Kwak and J. W. Park, Sensors, 2010, 10, 428–455.

5 (a) S. M. Hanash, *Electrophoresis*, 2000, ***21***, 1202–1209; (b) K. A. Baggerly, J. S. Morris and K. R. Coombes, *Bioinformatics*, 2004, ***20***, 777-785; (c) J. D. Wulfkuhle, L. A. Liotta and E. F. Petricoin, *Nat. Rev. Cancer*, 2003, ***3***, 267–275.

6 (a) N. D. B. Le, M. Yazdani and V. M. Rotello, *Nanomedicine*, 2014, ***9***, 1487–1498; (b) Y. Geng, W. J. Peveler and V. M. Rotello, *Angew. Chemie - Int. Ed.*, 2019, ***58,*** 5190–5200; (c) Y. Tao, X. Ran, J. Ren and X. Qu, *Small*, 2014, ***10***, 3667–3671.

7 M. De, S. Rana, H. Akpinar, O. R. Miranda, R. R. Arvizo, U. H. F. Bunz and V. M. Rotello, *Nat. Chem.*, 2009, ***1***, 461–465.

8 A. T. Wright, Z. Zhong and E. V. Anslyn, *Angew. Chem. Int. Ed.*, 2005, ***44***, 5679–5682.

9 Y. Geng, H. L. Goel, N. B. Le, T. Yoshii, R. Mout, G. Y. Tonga, J. J. Amante, A. M. Mercurio and V. M. Rotello, *Nanomedicine Nanotechnology, Biol. Med.*, 2018, **14**, 1931–1939.

10 (a) J. Han, M. Bender, K. Seehafer and U. H. F. Bunz, *Angew. Chem. Int. Ed.*, 2016, ***55***, 7689–7692; (b) J. Han, B. Wang, M. Bender, S. Kushida, K. Seehafer and U. H. F. Bunz, *ACS Appl. Mater. Interfaces*, 2017, ***9***, 790–797; (c) J. Han, B. Wang, M. Bender, K. Seehafer and U. H. F. Bunz, *Analyst*, 2017, ***142***, 537–543.

11 A. St John and C. P. Price, *Clin. Biochem. Rev.*, 2014, ***35***, 155 167.

12 (a) J. Han, B. Wang, M. Bender, K. Seehafer and U. H. F. Bunz, *ACS Appl. Mater. Interfaces*, 2016, ***8***, 20415–20421; (b) D. T. McQuade, A. E. Pullen and T. M. Swager, *Chem. Rev.*, 2000, ***100***, 2537–2574.

13 (a) S. Werner, H. Chen, J. Butt, A. Michel, P. Knebel, B. Holleczek, I. Zörnig, S. B. Eichmüller, D. Jäger, M. Pawlita, T. Waterboer and H. Brenner, *Sci. Rep.*, 2016, ***6***, 25467; (b) H. I. Yoon, O. R. Kwon, K. N. Kang, Y. S. Shin, H. S. Shin, E. H. Yeon, K. Y. Kwon, I. Hwang, Y. K. Jeon, Y. Kim and C. W. Kim, *J. Cancer Prev.*, 2016, ***21***, 187–193.

14 B. Heilig, M. Hüfner, B. Dörken and H. Schmidt-Gayk, *Klin. Wochenschr.*, 1986, ***64***, 776–780.

15 D. E. Shapiro, *Stat. Methods Med. Res.*, 1999, ***8***, 113–134.

16 A.-M. Šimundić, *EJIFCC*, 2009, ***19***, 203–211.

17 H. I. Maibach and F. Gorouhi in *Evidence Based Dermatology,* People's Medical House USA Ltd (PMPH), Shelton, Connecticut, 2011.